RESEARCH ARTICLE | NOVEMBER 26 2024

When can flexible weak polyelectrolytes be treated as effective rigid objects?

Javier Orradre ; Pablo M. Blanco ; Sergio Madurga ; Francesc Mas ; Josep Lluís Garcés

J. Chem. Phys. 161, 204906 (2024)
https://doi.org/10.1063/5.0233986

The Journal of Chemical Physics ARTICLE pubs.aip.org/aip/jcp

When can flexible weak polyelectrolytes be treated as effective rigid objects?

Cite as: J. Chem. Phys. 161, 204906 (2024); doi: 10.1063/5.0233986
Submitted: 19 August 2024 • Accepted: 5 November 2024 •
Published Online: 26 November 2024

Javier Orradre,[1,a] Pablo M. Blanco,[1,2] Sergio Madurga,[1] Francesc Mas,[1,b] and Josep Lluís Garcés[3,c]

AFFILIATIONS

[1] Department of Material Science and Physical Chemistry and Institute of Theoretical and Computational Chemistry (IQTC), University of Barcelona, Barcelona, Catalonia, Spain
[2] Department of Physics, Faculty of Natural Sciences, Norwegian University of Science and Technology (NTNU), Trondheim, Norway
[3] Department of Chemistry, Physics and Environmental and Soil Sciences and Agrotecnio, University of Lleida, Lleida, Catalonia, Spain

[a] **Author to whom correspondence should be addressed:** j.orradre@ub.edu
[b] **Electronic mail:** fmas@ub.edu
[c] **Electronic mail:** joseplluis.garces@udl.cat

ABSTRACT

Conformational and ionization equilibria of flexible weak polyelectrolytes (PEs) are, in general, strongly coupled. In this article, we analyze the effect of averaging over (or "contracting") the conformational degrees of freedom so that the original flexible molecule is replaced by an effective rigid object with the same ionization properties. As a result, one obtains the so-called Site Binding (SB) model, much easier to treat both theoretically and computationally, and extensively used to characterize the ionization properties of PE. The conformational averages can be performed in a systematic way by means of the Conformational Contraction Equations (CCEs), which relate the SB parameters to the underlying conformational equilibrium. The conditions for the convergence of the CCE are evaluated in the presence of both Short Range (SR) and Long Range (LR) electrostatic interactions. Two analytically solvable models based on the Freely Jointed Chain (FJC), involving only SR interactions, are analyzed at first. Despite the large chain flexibility, the resulting SB model reproduces the ionization properties with high accuracy. In the case of independent bonds, a very flexible chain can be *exactly* replaced by an effective rigid object with neighboring pairwise interactions. In general, however, triplet and higher order interactions emerge at the SB level. When LR electrostatic interactions are introduced and combined with the FJC large chain flexibility, the convergence of the CCE for long chains becomes problematic since the SB free energy must be truncated. Similar conclusions are reached for the freely rotating chain and rotational isomeric state models.

I. INTRODUCTION

The study of the ionization properties of polyprotic molecules and weak polyelectrolytes (PEs) largely relies on the analysis of the degree of protonation of the ionizable sites as a function of the pH-value, ionic strength, and temperature, among other variables. This quantity can be experimentally determined with high precision using potentiometry, spectrometry, or nuclear magnetic resonance (NMR).[1,2] The latter allows for not only the determination of the average degree of protonation but also that of the individual sites.[3,4] In order to extract thermodynamic information (protonation constants and interaction energies) from these experiments, the molecule is usually treated as a set of interacting sites, which can adopt two possible states: protonated or deprotonated. In this approach, which has been encompassed under the name of Site Binding (SB),[3,5–13] the underlying conformational degrees of freedom are not explicitly considered. In this way, the system complexity, the number of parameters, and the computational times are drastically reduced, facilitating the use of standard fitting procedures to obtain information about the ionization properties of the molecule of study.[2]

However, PEs are in general flexible macromolecules in which conformational and ionization states are strongly coupled[1,11,12,14–16] as protonation constants and interaction energies depend on the

conformational state. Therefore, the parameters from the SB level of description must be interpreted as implicit averages over the conformational degrees of freedom of the PE.[17] The SB approach can thus be regarded as an "effective" rigid object with the same ionization properties as the flexible chain.

Notwithstanding, this connection between the SB interaction energies and the molecular geometry has been usually based on heuristic assumptions. For instance, a rather popular approach is to treat linear PE chains as rigid rods.[18–25] The underlying argument holds that charged PEs tend to be in extended conformations, an arrangement that can be approximated as a set of charges located on a cylinder. This approximation plays an essential role in Manning's counterion condensation theory,[26–36] in the cell model of concentrated PE solutions,[37–40] or in the study of PE–PE interactions.[41] The main objection to the rod approximation is that PEs are essentially coils at low charge densities, and fluctuations in the monomer orientations occur even at intermediate charge densities.[21,22,42,43] Models making use of the coil approximation can be found in the classical studies by Katchalsky *et al.*,[44] Harris and Rice,[45] or in the so-called living random coil approximation.[46,47] However, the transition from coil to rod is smooth in general, and it is not clear to assign one of the two geometries at pH values where the PE is partially ionized.

The key aspect to address is thus as follows: "Given a full conformation–protonation description, how the conformational degrees of freedom must be averaged to obtain the SB parameters?". The answer is found in the equations originally published in Ref. 17, to which we refer as "Conformational Contraction Equations" (CCEs).

The procedure through which a flexible PE molecule is transformed into an effective rigid object is outlined in Fig. 1. At first, the protonation and conformation equilibria are coupled since changes in the conformational state modify the electrostatic interactions between charged sites, inducing a shift in the protonation equilibria. In turn, changes in the protonation state affect the conformational energy. We refer to this complete picture as the Coupled Conformational Site Binding (CCSB) level of description, where both protonation and conformation equilibria are treated on equal footing. In particular, when the conformational equilibrium is described by means of Flory's Rotational Isomeric State (RIS) model, we obtain the SBRIS model.[4,13,17,48] In the same figure, it is shown that by applying the CCEs to the CCSB description, the conformations are averaged over and the equivalent SB model is obtained.

The CCE approach has successfully explained the conformational transition in polymethacrylic acid (PMA)[17] and the emergence of three-body interactions in polyethylenimines (LPEI).[48,49] However, a study of the conditions under which a flexible polyprotic molecule can be described as an effective rigid object within the SB framework by means of the CCE is still lacking and constitutes the main objective of this work.

This article is organized as follows: In Sec. II, the conformational contraction equations, which provide the parameters of the SB level in terms of the underlying CCSB level, are presented. In Sec. III, the SB treatment is applied to PE models, which include only Short Range (SR) interactions. In the absence of sharp conformational transitions, the SB free energy rapidly converges despite the high flexibility of the chain. The role of Long Range (LR) interactions is investigated in Sec. IV. As will be shown, in the presence of LR interactions, the convergence of the SB model is problematic for long and highly flexible chains. Finally, the main conclusions are summarized in Sec. V.

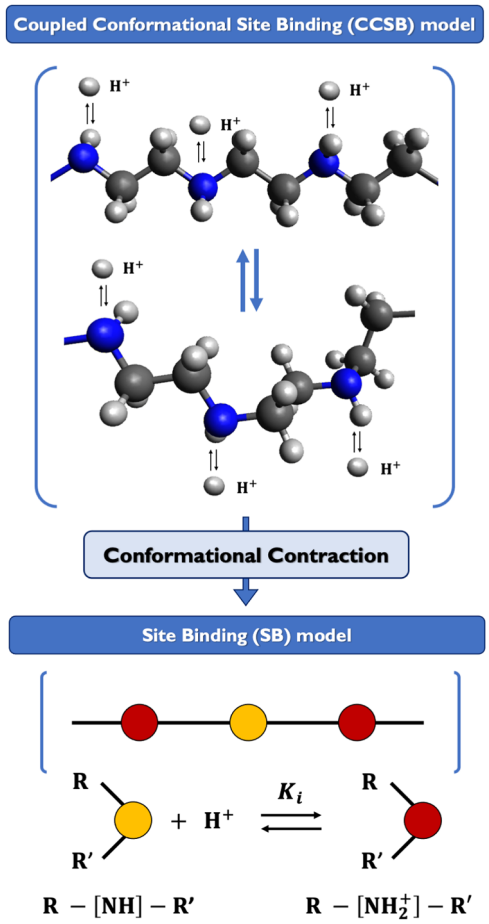

FIG. 1. Outline showcasing the averaging procedure over the conformational degrees of freedom using the Conformational Contraction Equations (CCEs). The PE (LPEI as an example) is a flexible object with strongly coupled conformational and protonation states. This full description is referred to as Coupled Conformational Site Binding (CCSB) level. When performing the contraction with the CCE, an effective rigid object is obtained with the same ionization properties as the underlying flexible one. This corresponds to the Site Binding (SB) level of description.

II. FLEXIBLE POLYPROTIC MOLECULES AS EFFECTIVE RIGID OBJECTS

A. Site Binding (SB) model

The Site Binding model represents a polyprotic molecule as a set of N ionizable groups, which can be either protonated or deprotonated (Fig. 1). Without loss of generality, we will identify the charged state as the protonated one, while the deprotonated state is neutral. This is the case of polybases such as polyamines. The following discussion, however, can be readily extended to polyacids

or polyampholytes.[2] The ionization state of the macromolecule is characterized by a set of state variables $s = \{s_i, \quad i = 1, \ldots N\}$, where $s_i = 1$ if the site i is protonated and $s_i = 0$ if it is deprotonated. The free energy is expressed in terms of the cluster expansion[50] as

$$F_{\mathrm{SB}}(s) = \sum_i \tilde{\mu}_i s_i + \sum_{j>i} \tilde{\varepsilon}_{ij} s_i s_j + \sum_{k>j>i} \tilde{\lambda}_{ijk} s_i s_j s_k + \cdots, \tag{1}$$

where $\tilde{\mu}_i = \mathrm{k_B}T \ln 10\ (\mathrm{pH} - \log \widetilde{K}_i)$ is the reduced chemical potential of site i and $\widetilde{K}_i$ refers to the protonation constant of site i; $\tilde{\varepsilon}_{ij}$ represents the pair interaction energy between protonated sites i and j; and $\tilde{\lambda}_{ijk}$ is the triplet (three-body) interaction among sites i, j, and k, and so on. These interactions must be interpreted as excess energies, in the sense that, for instance, $\tilde{\lambda}_{ijk}$ is a correction to $\tilde{\varepsilon}_{ij}$, $\tilde{\varepsilon}_{jk}$, and $\tilde{\varepsilon}_{ik}$. In the SB level, the molecule is treated as an effective rigid object, since no reference to the conformational states is made. In order to deal with the coupling of conformations and protonation, one needs to extend the free energy of Eq. (1) to explicitly include the conformational contribution.

B. Coupling of conformation and protonation equilibria: Coupled Conformational Site Binding (CCSB) model

Let us consider that our PE can also adopt a number of conformational states resulting from the internal stretching, bending, and rotation of the bonds. As a result, the chemical potentials and interaction energies depend on the conformational state c and the free energy reads

$$F_{\mathrm{CCSB}}(s,c) = F_{\mathrm{ref}}(c) + F_{\mathrm{P}}(s,c) = F_{\mathrm{ref}}(c) + \sum_i \mu_i(c) s_i + \sum_{j>i} \varepsilon_{ij}(c) s_i s_j + \sum_{k>j>i} \lambda_{ijk}(c) s_i s_j s_k + \cdots, \tag{2}$$

where the term $F_{\mathrm{ref}}(c)$ represents the conformational free energy of the fully deprotonated (uncharged) molecule, which is regarded as the reference state. The functional form of this term will vary depending on the conformational properties of the specific model. Note that the reduced chemical potential $\mu_i(c) = \mathrm{k_B}T \ln 10\ (\mathrm{pH} - \log K_i(c))$ and the protonation constant depend on the conformational state, due to the changes induced in the chemical environment of the sites. The previous equation actually defines the CCSB level of description.

Clearly, the number of parameters involved in the CCSB free energy [Eq. (2)] is much larger than the one used in the SB level of description [Eq. (1)]. Moreover, in many cases, the dependence of reduced chemical potentials and interaction energies on the conformation can be very complicated, especially for large molecules. Since the aim is to fit the free energy parameters to potentiometric or NMR titrations, most of the quantitative studies rely on the SB approach,[2,51–54] while studies using the CCSB level of description are scarce.[48,55] However, it is implicit in working at the SB level that $\tilde{\varepsilon}_{ij}$, $\tilde{\lambda}_{ijk}$, and so on, in Eq. (1) should be regarded as some type of conformational average of $\mu_i(c)$, $\varepsilon_{ij}(c)$, $\lambda_{ijk}(c)$, etc., from Eq. (2). Such an averaging or "contraction" process is not trivial, and it is the subject of Subsection II C.

C. Connection between the CCSB and SB descriptions: Conformational Contraction Equations (CCEs)

The crucial link between the free energies of the SB and CCSB levels is given by[17]

$$e^{-\beta F_{\mathrm{SB}}(s)} = \left\langle e^{-\beta F_{\mathrm{P}}(s,\,c)} \right\rangle_{\mathrm{ref}}, \tag{3}$$

where the average is taken over the conformational energies of the reference state (i.e., the uncharged molecule). A detailed derivation of Eq. (3) is provided in Sec. S-1 of the supplementary material. Since the average is not performed over the free energies but over their Boltzmann factors, it is convenient to define the following quantities:

$$z_i(c) = e^{-\beta \mu_i(c)}; \quad u_{ij}(c) = e^{-\beta \varepsilon_{ij}(c)}; \quad w_{ijk}(c) = e^{-\beta \lambda_{ijk}(c)}. \tag{4}$$

By equating terms corresponding to the same protonation state on both sides of Eq. (3), the contracted parameters of the SB level can be expressed as averages of the CCSB energies over the reference state,

$$\tilde{z}_i = e^{-\beta \tilde{\mu}_i} = \left\langle e^{-\ln 10\ (\mathrm{pH} - \log K_i(c))} \right\rangle_{\mathrm{ref}} = \langle z_i(c) \rangle_{\mathrm{ref}}, \tag{5}$$

$$\tilde{u}_{ij} = e^{-\beta \tilde{\varepsilon}_{ij}} = \frac{\langle z_i(c) z_j(c) u_{ij}(c) \rangle_{\mathrm{ref}}}{\tilde{z}_i \tilde{z}_j}, \tag{6}$$

$$\tilde{w}_{ijk} = e^{-\beta \tilde{\lambda}_{ijk}} = \frac{\left\langle z_i(c) z_j(c) z_k(c) u_{ij}(c) u_{ik}(c) u_{jk}(c) w_{ijk}(c) \right\rangle_{\mathrm{ref}}}{\tilde{z}_i \tilde{z}_j \tilde{z}_k \tilde{u}_{ij} \tilde{u}_{ik} \tilde{u}_{jk}}. \tag{7}$$

Expressions for higher order interactions (quadruplets, quintuplets, etc.) are obtained in the same way. They represent the sought Conformational Contraction Equations (CCEs) for the SB parameters as first derived in Ref. 17. An alternative, perhaps simpler, derivation is provided in Sec. S-2 of the supplementary material. Note that the structure of the CCE is recursive. For instance, to obtain the SB triplet interactions, the SB chemical potential and pairwise interactions are necessary.

Besides their rather non-trivial form, some relevant and even counterintuitive aspects of the CCE are worth to comment. First, the fact that the averages in Eqs. (5)–(7) are over the reference state means that the ionization properties can be calculated using the conformation statistics of the *uncharged* molecule, usually much simpler to deal with. Second, when triplet interactions are neglected at the CCSB level, i.e., $\lambda_{ijk}(c) = 0$, the triplet contracted parameters $\tilde{\lambda}_{ijk}$ do not vanish,

$$\beta \tilde{\lambda}_{ijk} = -\ln \tilde{w}_{ijk} = -\ln \frac{\left\langle z_i(c) z_j(c) z_k(c) u_{ij}(c) u_{ik}(c) u_{jk}(c) \right\rangle_{\mathrm{ref}}}{\tilde{z}_i \tilde{z}_j \tilde{z}_k \tilde{u}_{ij} \tilde{u}_{ik} \tilde{u}_{jk}} \neq 0, \tag{8}$$

which means that triplet interactions, which are not present at the CCSB level, can arise at the SB level due to conformational effects. The emergence of triplet interactions has been experimentally reported for polyethylenimines (LPEI) of different sizes and

structures[9,49] and for polyphosphate acids.[7] A very detailed analysis of the LPEI case can be found in Ref. 48.

D. Methodology

In order to test the accuracy and convergence of the CCE, which is the main objective of this work, the subsequent steps have been followed:

(i) A Coupled Conformational Site Binding (CCSB) model is proposed, whose titration curves are obtained either analytically or by simulations. The CCSB models analyzed in this work are depicted in Fig. 2. For the Four-State Model (4-SM) and the Freely Jointed Chain (FJC) with SR interactions, exact analytical solutions are available. However, when LR interactions are included in the FJC, the Freely Rotating Chain (FRC), and the Rotational Isomeric State (RIS) models, Semi-Grand Canonical Monte Carlo (SGCMC) simulations need to be performed. In SGCMC simulations, the pH-value is kept constant, while the number of bound protons fluctuates.[46] The Metropolis–Hastings algorithm[56,57] is applied to the free energy from Eq. (2). These SGCMC simulations are usually very time consuming (of the order of days for a single titration curve).

(ii) By means of the CCE, the SB parameters and the titration curves corresponding to the equivalent rigid system are obtained. When only SR interactions are considered in the model, the CCE can be analytically evaluated. For the models including LR interactions, the averages over the reference state can only be analytically calculated in the case of the FJC. In the rest of models, specific MC simulations in the canonical ensemble must be performed.

(iii) Once the SB contracted energies are available, the SB titration curve is obtained either analytically or by SGCMC simulations depending on the case. Since conformations are absent at the SB level [Eq. (1)], these simulations are very fast (a few seconds for a single titration curve).

(iv) Finally, the CCSB and SB titration curves are compared and the convergence of the CCE is analyzed.

A detailed outline of the full procedures (i)–(iv) for each model and the computational details are provided in Secs. S-3 and S-4 of the supplementary material.

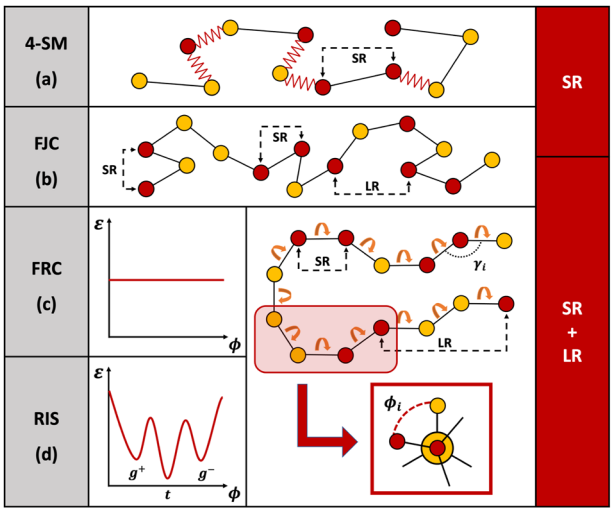

FIG. 2. Outline of the models considered in the present work: (a) Four-State Model (4-SM), where the bonds can adopt two possible conformations ("short" and "long") with different energies; (b) Freely Jointed Chain (FJC) with Short Range (SR) and Long Range (LR) interactions: in the uncharged chain, the bond orientation is random and independent; (c) Freely Rotating Chain (FRC): bond angles γ_i are fixed and dihedral angles (ϕ_i) rotate with an independent conformational energy; and (d) Rotational Isomeric State (RIS) model: bond angles γ_i are fixed too and the presence of rotational barriers leads to the predominant population of three states, namely *trans* ($t, \phi_i = 180°$), *gauche*$^+$ ($g^+, \phi_i = 60°$), and *gauche*$^-$ ($g^-, \phi_i = -60°$).

III. SHORT RANGE INTERACTIONS

First, let us consider the situation in which only nearby sites interact, namely, only Short Range (SR) interactions are relevant. This is the case at high ionic strengths for which the SB model has been extensively used.[3–6,8,11–13] Moreover, for linear molecules, the SR models can be analytically solved by means of transfer matrix techniques.[58] The models discussed in this work are depicted in Fig. 2, all of them consisting in linear chains with N identical sites and protonation constants independent of the conformational state [i.e., $\mu_i(c) = \mu$].

A. Freely Jointed Chain (FJC) with rigid bonds and nearest and next-nearest neighbor interacting sites

In this model, the chain consists of a set of bonds of fixed length b whose orientation is statistically independent when the chain is uncharged. The site–site interaction energies are given by the Debye–Hückel (DH) potential at a given ionic strength I. Nearest neighbor (NN) sites interact with a conformation independent energy ε_n (due to the fixed bond distance), while next-nearest neighbor (NNN) sites interact at a distance $r_{nn}(\gamma_i)$ according to

$$\beta\varepsilon_{ij}(r_{ij}) = \frac{\ell_B}{r_{ij}} \exp(-r_{ij}/\ell_D), \tag{9}$$

$$r_{i,i+2} = r_{nn}(\gamma_i) = b\sqrt{2(1-\cos(\gamma_i))}, \tag{10}$$

where γ_i is the angle between two consecutive bonds, $\ell_D = \sqrt{\varepsilon k_B T/2N_A e^2 I}$ is the Debye length, $\ell_B = e^2/4\pi\varepsilon k_B T$ is the Bjerrum length, ε is the permittivity of the medium (in this work, water at 20 °C), e is the electron charge, and N_A is Avogadro's number. A particular conformation is defined as the set of angles $\gamma = \{\gamma_1, \gamma_2, \ldots, \gamma_{N-2}\}$. A sketch of the system is depicted in Fig. 2(b). This model can be analytically solved at the CCSB level by using transfer matrices, and exact expressions are available for both the degree of protonation and the end-to-end distance. The resulting equations and derivations are provided in Ref. 59.

The degree of protonation and the end-to-end distance vs the pH-value are depicted in Figs. 3(a) and 3(b), respectively, for different ionic strengths. As can be observed, the end-to-end distance increases as the pH-value decreases due to the increase in molecular charge, indicating that conformation and protonation equilibria

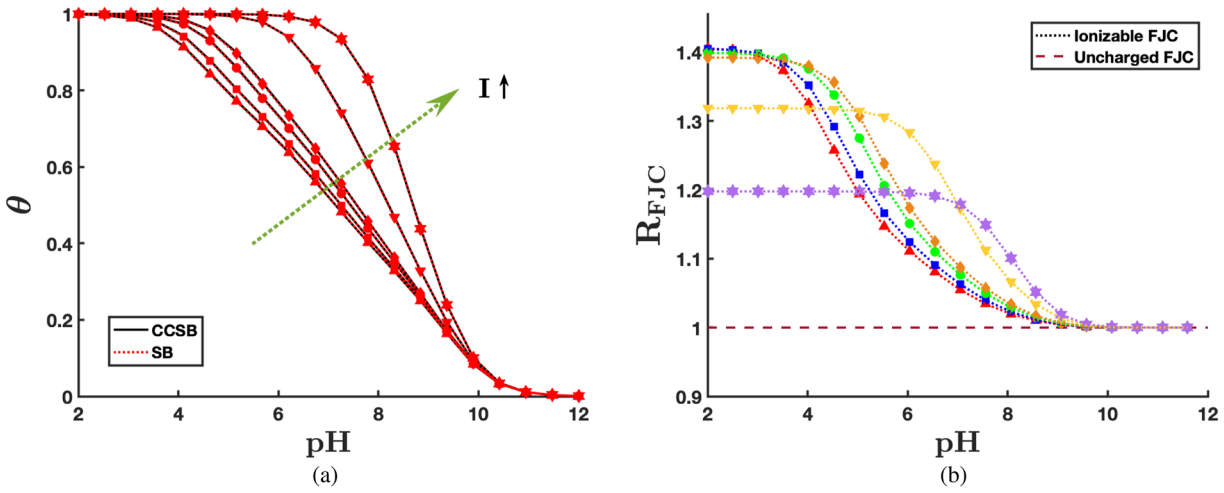

FIG. 3. FJC model with rigid bonds of length $b = 0.25$ nm, $\log K = 9.0$, and $N = 20$ monomers. Only SR nearest and next-nearest neighbor interactions are considered, described by the DH potential. (a) Titration curves corresponding to the CCSB flexible chain (black) and the equivalent SB model (red), which exactly match. (b) End-to-end distance normalized to that of the uncharged FJC, $R_{\mathrm{FJC}} = \sqrt{\langle r^2\rangle/(N-1)b^2}$, vs pH. The ionic strengths used are: 0.001M (upward triangles), 0.01M (squares), 0.05M (circles), 0.1M (diamonds), 1M (downward triangles), and 5M (stars). For the sake of data visibility, different colors have also been used in the end-to-end distance.

are strongly coupled.[59] This swelling effect is more pronounced at low ionic strengths, due to stronger repulsion between charged sites. The end-to-end distance increases from the value corresponding to the uncharged FJC at large pH-values ($R_{\mathrm{FJC}} = \sqrt{\langle r^2\rangle/(N-1)b^2}$) until a plateau corresponding to the fully protonated molecule is formed at low enough pH-values. Note that even though the PE is fully charged, the end-to-end distance does not achieve the contour length due to thermal fluctuations in the bond angles.

The key point is that, despite being a very flexible chain, this system can be *exactly* replaced by an equivalent rigid system, which is a rather surprising result. As a result, the SB and CCSB titration curves coincide, as can be observed in Fig. 3(a), which can be explained as follows.

Using the CCE and performing the necessary averages over the reference state, it is immediate to verify that the SB interaction energy for NN sites is $\tilde{\varepsilon}_{\mathrm{n}} = \varepsilon_{\mathrm{n}}$ due to the fixed bond length. For NNN sites, the average over the angles renders $\tilde{\varepsilon}_{\mathrm{nn}}$ as

$$\beta\tilde{\varepsilon}_{\mathrm{nn}} = \ln\left\{\frac{1}{2}\int_0^{\pi} \exp\left(-\beta\varepsilon_{\mathrm{nn}}(\gamma)\right)\sin(\gamma)d\gamma\right\}. \tag{11}$$

Since $\varepsilon_{ij}(c) = 0$ for $|j-i| > 2$ and $\lambda_{ijk}(c) = 0$ at the conformational level, $\tilde{\varepsilon}_{ij} = 0$ for $|j-i| > 2$ and $\tilde{\lambda}_{ijk} = 0$. Higher order interactions also vanish.

As a result, the CCEs yield a SB model consisting of a set of identical sites with NN and NNN interaction energies, $\tilde{\varepsilon}_{\mathrm{n}}$ and $\tilde{\varepsilon}_{\mathrm{nn}}$, respectively, which can be analytically solved using transfer matrices.[59,60] The fact that the SB free energy terminates at neighboring pairwise interactions is a rather counterintuitive result. Due to the conformation–protonation coupling, the binding states become increasingly correlated at larger distances as the bond angles increase and the PE swells. Therefore, one would expect LR and many-body interactions to emerge at the SB level. However, the CCEs predict that this is not the case, a fact that has been experimentally observed for PAA.[17]

B. FJC with two possible bond conformations: Four-State Model (4-SM)

Let us here go one step further introducing flexible bonds that can adopt two different conformations: "short" (S) and "long" (L), with bond lengths b_{S} and b_{L}, respectively. Considering the L conformation as the zero energy level, the energy of the S conformation and the corresponding Boltzmann factor are denoted as $\rho_{\mathrm{S}} = -\mathrm{k_B}T\ln\sigma$. Two consecutive bonds are no longer independent, and we denote the interaction energy of two adjacent S-bonds as $\rho_{\mathrm{SS}} = -\mathrm{k_B}T\ln\psi$. If $\psi < 1$, two adjacent S conformations are hindered, while for $\psi > 1$, S conformations tend to appear together. Possible negative or positive cooperativity between consecutive S-bonds is thus considered. An outline of the model can be found in Fig. 2(a), and the conformational energy $F_{\mathrm{ref}}(c)$ is defined as follows:

$$F_{\mathrm{ref}}(c) = \rho_{\mathrm{S}}\sum_{i}^{N-1} l_i + \rho_{\mathrm{SS}}\sum_{i}^{N-1} l_i l_{i+1}, \tag{12}$$

where $l = \{l_i, i = 1, \ldots N-1\}$ is the set of bond states, being $l_i = 1$ if the bond i is in the S conformation or $l_i = 0$ if it is in the L one.

Protonation is mediated through $\mu = -\mathrm{k_B}T\ln z$, and only NN electrostatic interactions, which depend on the conformational state of the linking bond (L or S), are considered. They are denoted as $\varepsilon_{\mathrm{L}} = -\mathrm{k_B}T\ln u_{\mathrm{L}}$ and $\varepsilon_{\mathrm{S}} = -\mathrm{k_B}T\ln u_S$, and they are responsible for the coupling between conformations and protonation in this model. As a result, the basic unit of the chain (a site plus a bond) can adopt four possible states, so we refer to this model as "Four-State Model" (4-SM) following previous publications.[17,48] The resulting CCSB model can be exactly solved by using the transfer matrix

$$\mathbf{T} = \begin{pmatrix} 1 & \sigma & z & z\sigma \\ 1 & \sigma\psi & z & z\sigma\psi \\ 1 & \sigma & zu_{\mathrm{L}} & z\sigma u_{\mathrm{S}} \\ 1 & \sigma\psi & zu_{\mathrm{L}} & z\sigma\psi u_{\mathrm{S}} \end{pmatrix}. \tag{13}$$

Despite its simplicity, this model has been key to studying the coupling between binding and conformations of LPEI[48] and the sharp conformational transition of PMMA.[17] For this 4-SM case, the mean square end-to-end distance reads

$$\frac{\langle r^2 \rangle}{(N-1)} = P_{\mathrm{L}}(\mathrm{pH}) b_{\mathrm{L}}^2 + P_{\mathrm{S}}(\mathrm{pH}) b_{\mathrm{S}}^2, \tag{14}$$

which is pH-dependent via the L and S bond state probabilities P_{L} and P_{S}, respectively, whose detailed expressions are provided in the supplementary material (Sec. S-6.2). The titration curves, end-to-end distances, and bond state probabilities are shown in Fig. 4 for three different situations: independent, repulsive, and attractive interactions between adjacent bonds in the S state. As expected, the molecule swells as the pH-value decreases, as reflected by the increase in both the end-to-end distance and the L bond state probability. The molecule is thus very flexible in all the cases.

Using the CCE, it is found that in the absence of bond–bond interactions ($\sigma = 1, \psi = 1$), triplet and higher order interactions vanish at the SB level. Thus, despite its large flexibility, the molecule can be *exactly* mapped on an equivalent rigid object with effective

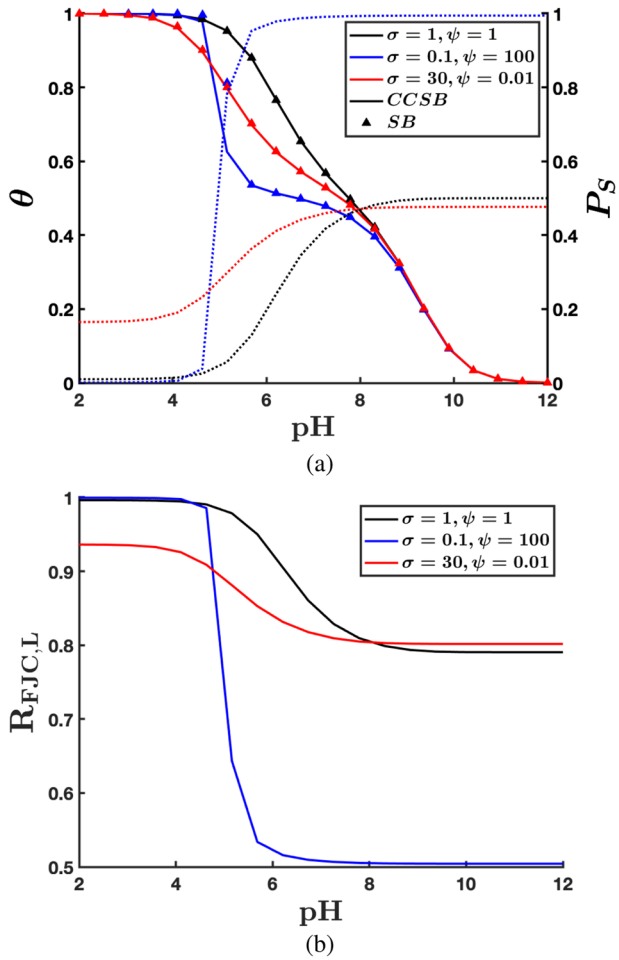

FIG. 4. Four-State Model (4-SM) with $N = 50$, $\log K = 9.0$, $u_{\mathrm{L}} = 0.1$, $u_{\mathrm{S}} = 0.001$, $b_{\mathrm{L}} = 0.4$ nm, and $b_{\mathrm{S}} = 0.2$ nm. (a) Degree of protonation (CCSB with solid lines and SB with markers) and S bond probability P_{S} (dotted lines) vs pH. (b) End-to-end distance normalized to that of the uncharged FJC with bond distance b_{L}, $R_{\mathrm{FJC,L}} = \sqrt{\langle r^2 \rangle/(N-1)b_{\mathrm{L}}^2}$, vs pH. Three cases are considered: $\sigma = 1$, $\psi = 1$ (black); $\sigma = 0.1$, $\psi = 100$ (blue); and $\sigma = 30$, $\psi = 0.01$ (red). Degree of protonation of the equivalent rigid system (SB) using up to quintuplet interactions.

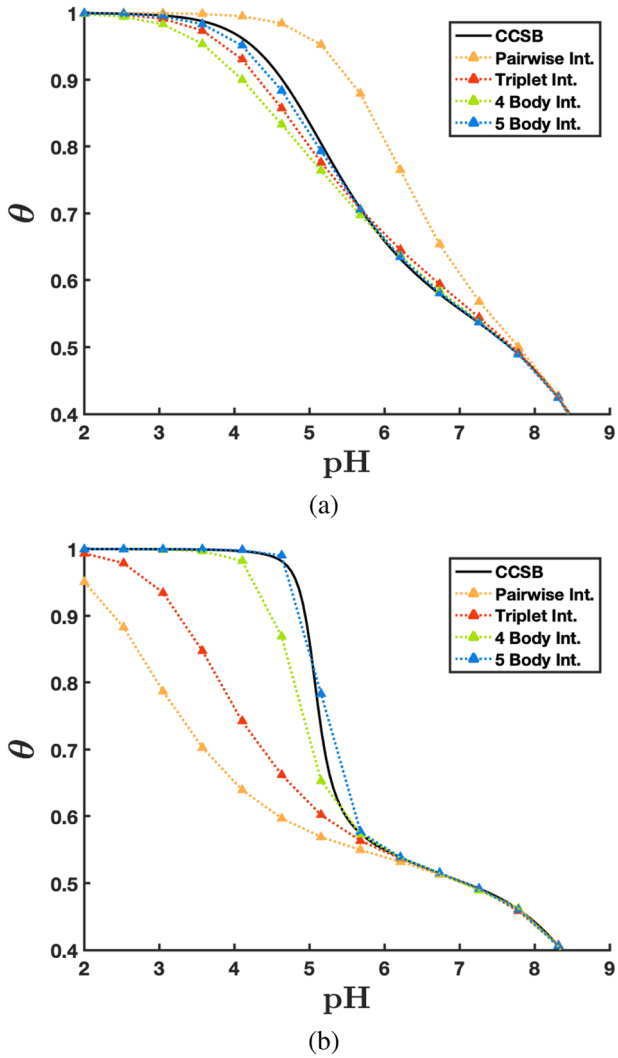

FIG. 5. Convergence of the SB model to the Four-State CCSB model. Degree of protonation corresponding to the exact solution (black solid line) and to the equivalent rigid object (markers) considering pairwise (yellow), triplet (red), quadruplet (green), and quintuplet (blue) interactions vs pH for a chain with $N = 20$, $\log K = 9.0$, $u_t = 0.1$, $u_g = 0.001$, $b_{\mathrm{L}} = 0.4$ nm, $b_{\mathrm{S}} = 0.2$ nm and (a) $\sigma = 30$, $\psi = 0.01$ and (b) $\sigma = 0.1$, $\psi = 100$. Dotted lines connecting the markers are shown only for guidance.

pair interactions. The same conclusion was reached in the model of Subsection III A. Therefore, a rigid chain is not a necessary condition for the suitability of the SB approach.

In the presence of S bond–bond interactions, the CCEs lead to non-vanishing triplet and larger order interactions at the SB level. In Fig. 5, the exact CCSB titration curves from Fig. 4 are compared with the SB models progressively adding pairwise, triplet, quadruplet, and quintuplet interactions. In the case of repulsive bond–bond interactions [$\sigma = 30, \psi = 0.01$, Fig. 5(a)], the convergence is fast, albeit not necessarily monotonic (for instance, the SB model including triplet interactions provides a more precise titration curve than including quadruplet interactions). However, from a practical standpoint, triplet interactions are enough to reproduce very accurately the exact curve below the experimental error, as experimentally observed for LPEI.[48,49]

Finally, attractive S bond–bond interactions (case $\sigma = 0.1$, $\psi = 100$) can lead to drastic conformational transitions in a narrow range of pH-values, as observed in the S bond probability and the end-to-end distance in Fig. 4(b). Polymers such as PMMA experience these kinds of transitions.[61] It is shown that the CCE convergence is very slow [Fig. 5(b)], i.e., one needs to consider more terms in the SB free energy cluster expansion, due to the long correlations involved in the quasi-phase transition.

IV. LONG RANGE INTERACTIONS

So far, we have shown that when only SR interactions are present, the protonation properties of the original flexible PE can be described very accurately by an equivalent rigid object. Moreover, in the absence of sharp conformational transitions, the convergence of the CCE is fast and only triplet interactions are necessary to fully reproduce the titration curves. However, at intermediate and low ionic strengths, electrostatic LR interactions are unavoidable. Let us analyze this effect when the uncharged molecule behaves either as a Freely Jointed Chain (FJC), as a Freely Rotating Chain (FRC), or as a Rotating Isomeric State (RIS) model. These models are depicted in Fig. 2.

A. Freely Jointed Chain (FJC)

Consider that two protonated sites i and j, not necessarily neighbors, interact at a distance r_{ij} via the DH potential [Eq. (9)]. In this case, the corresponding SB model can be derived recalling that the CCEs only involve averages over the reference (uncharged) state. For a FJC, the probability distribution of distances r_{ij} $(0 \le r_{ij} \le mb)$ is given by

$$W_m^{\mathrm{T}}(r_{ij}) = \frac{\pi}{4} m(m-1) \sum_{t=0}^{\tau} \frac{(-1)^t}{t!(m-t)!} \left[\frac{m - \frac{r_{ij}}{b} - 2t}{2} \right]^{m-2}, \qquad (15)$$

where $m = |j - i| \ge 2$ and τ is the integer part of $(m - r/b)/2$. The distribution in Eq. (15), due to Treloar,[62] is far from being Gaussian for low m values, for which the electrostatic interactions are more intense (see Sec. S-7.1 of the supplementary material). For $m > 6$, however, it can be accurately approximated by a Gaussian because of the central limit theorem.[63]

Introducing Eq. (15) and the DH potential [Eq. (9)] in Eq. (6) and integrating over the angle variables, $\tilde{\varepsilon}_m$ reads

$$e^{-\beta\tilde{\varepsilon}_m} = \left\langle e^{-\beta\phi(r_{ij})} \right\rangle_{\mathrm{ref}} = \int_0^{mb} \exp\left[-\frac{\ell_{\mathrm{B}}}{r_{ij}} \exp\left(-r_{ij}/\ell_{\mathrm{D}}\right) \right] W_m^{\mathrm{T}}(r_{ij}) dr_{ij}. \qquad (16)$$

A very good approximation to Eq. (16) can be obtained by expanding the exponential term around the average value (A.V. Approx.), leading to

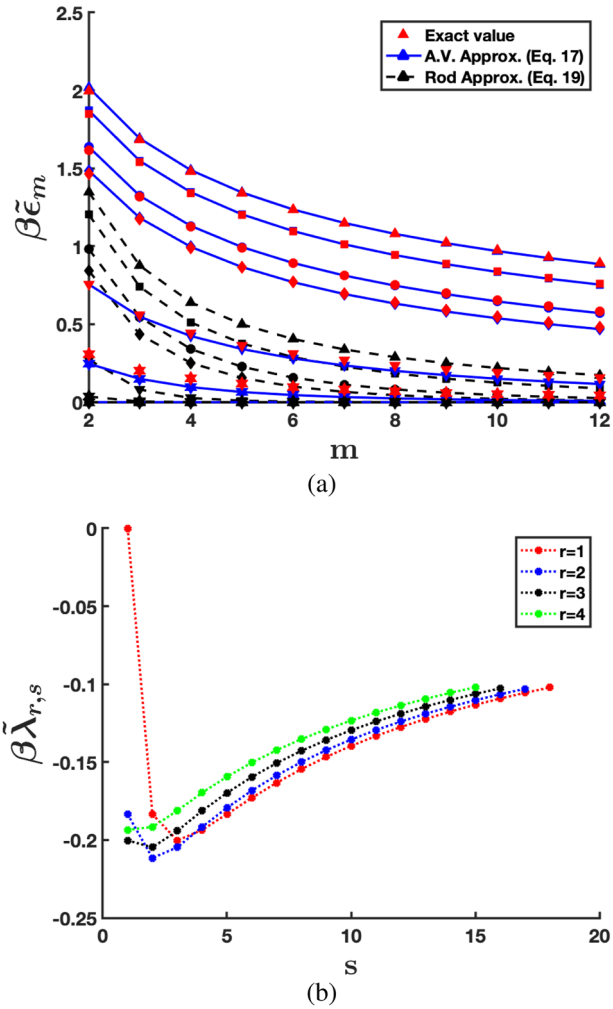

FIG. 6. (a) SB pair interactions $\tilde{\varepsilon}_{ij} = \tilde{\varepsilon}_m$ calculated using the FJC model [Eq. (16), red circles], the average value approximation [Eq. (17), blue solid lines], and the rod approximation [Eq. (19), black dashed lines] as a function of the separation between sites $m = |j - i|$. The chosen parameters are as follows: $b = 0.25$ nm, $\log K = 9.0$, and ionic strengths 0.001M (upward triangles), 0.01M (squares), 0.05M (circles), 0.1M (diamonds), 1M (downward triangles), and 5M (stars). (b) SB triplet interactions $\tilde{\lambda}_{ijk} = \tilde{\lambda}_{rs}$ (where $r = |j - i|$ and $s = |k - j|$) for the FJC with $b = 0.25$ nm, $\log K = 9.0$, and ionic strength 0.001M as a function of s for fixed $r = 1$ (red), $r = 2$ (blue), $r = 3$ (black), and $r = 4$ (green). Dotted lines connecting the markers are shown only for guidance.

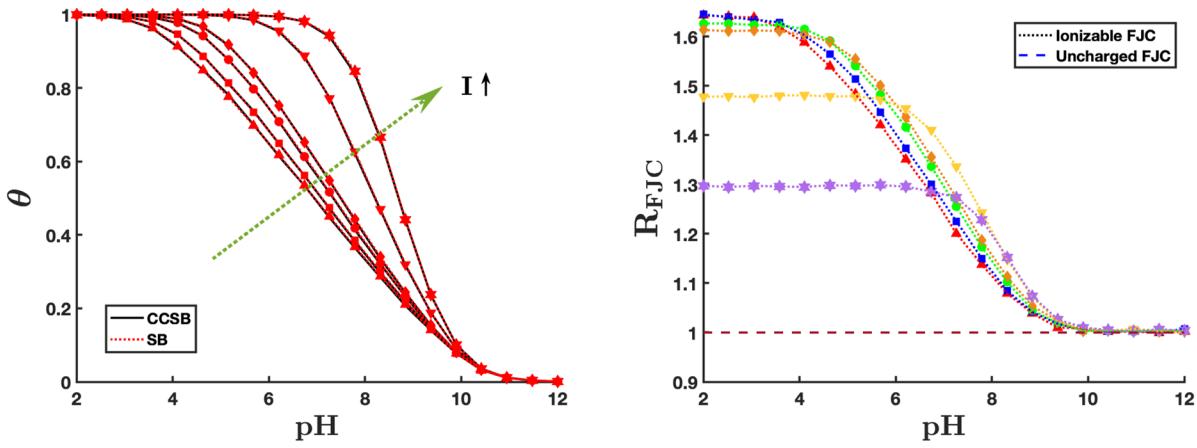

(a) $N = 6$

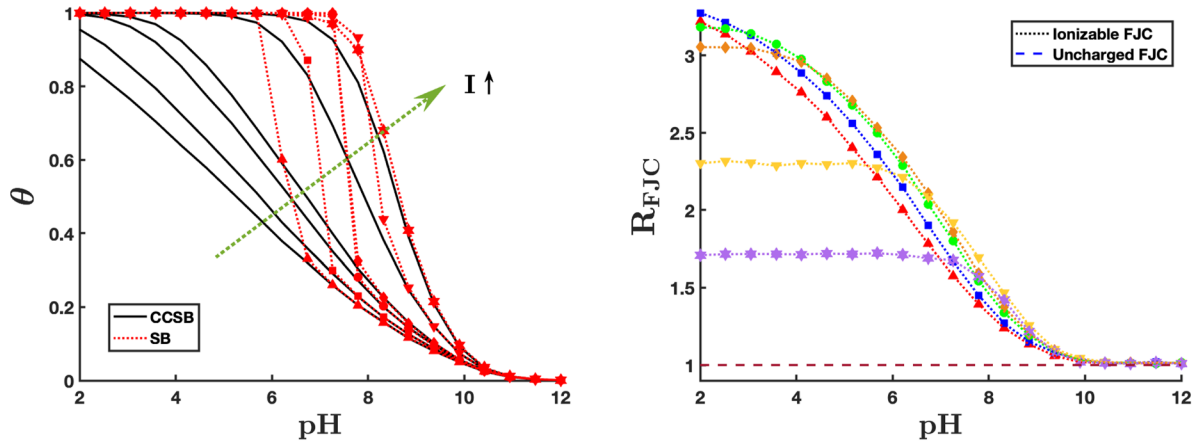

(b) $N = 20$

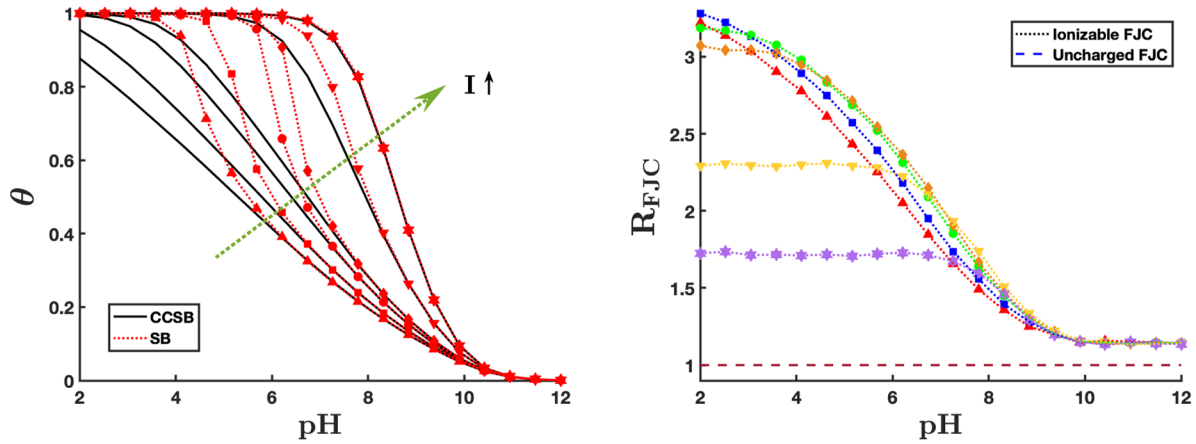

(c) $N = 20$ with Excluded Volume

FIG. 7. Left panels: titration curves of a flexible ionizable FJC (black) and the equivalent rigid SB system with pair and triplet interactions (red). Right panels: end-to-end distance vs pH-value. Cases shown are (a) $N = 6$, (b) $N = 20$, and (c) $N = 20$ adding excluded volume interactions (bead diameter $d = 0.1$ nm). In all the cases, $b = 0.25$ nm and $\log K = 9.0$. The ionic strengths used are 0.001M (upward triangles), 0.01M (squares), 0.05M (circles), 0.1M (diamonds), 1M (downward triangles), and 5M (stars). The end-to-end distance is normalized to that of the uncharged FJC, $R_{FJC} = \sqrt{\langle r^2 \rangle / (N-1)b^2}$, and to improve data visibility, different colors have been used for each ionic strength. Dotted lines connecting the markers are only for eye guidance.

$$\beta\tilde{\varepsilon}_m \approx \left[\frac{\ell_B}{\sqrt{m}b} + C(m)\right]\exp\left(-\sqrt{m}b/\ell_D\right) \tag{17}$$

with

$$C(m) = \frac{(m-1)}{12m}\frac{\ell_B}{b}\Big[\left(\sqrt{m}(b/\ell_D)^2 + 3(b/\ell_D) + 3/\sqrt{m}\right) - (\ell_B/b)\exp\left(-\sqrt{m}b/\ell_D\right)\left(b/\ell_D + 1/\sqrt{m}\right)^2\Big]. \tag{18}$$

Note that if the term $C(m)$ is set to zero, the DH energy with distance $\sqrt{m}b$ is obtained, which looks rather intuitive. However, numerical calculations show that this term cannot be neglected since it is of the same order of magnitude as $\ell_B/\sqrt{m}b$. The complete derivation is reported in the supplementary material (Sec. S-7.2). Nonetheless, the most significant finding is that the decay of $\tilde{\varepsilon}_m$ with m in Eq. (17) differs from the rod approximation, widely used in the literature,[2,21] which predicts a much faster decay,

$$\beta\tilde{\varepsilon}_m = \frac{\ell_B}{mb}\exp\left(-mb/\ell_D\right), \tag{19}$$

as can be observed in Fig. 6(a), where $\tilde{\varepsilon}_m$ vs m is depicted for different ionic strengths. Equations (16) and (17) illustrate the fact that, at low charges, when only pair interactions at the SB level are activated, the rod approximation is not appropriate because of the large chain flexibility.

At higher charges, SB triplet interactions $\tilde{\lambda}_{ijk}$ become important. Their calculation using the CCEs is similar, although the

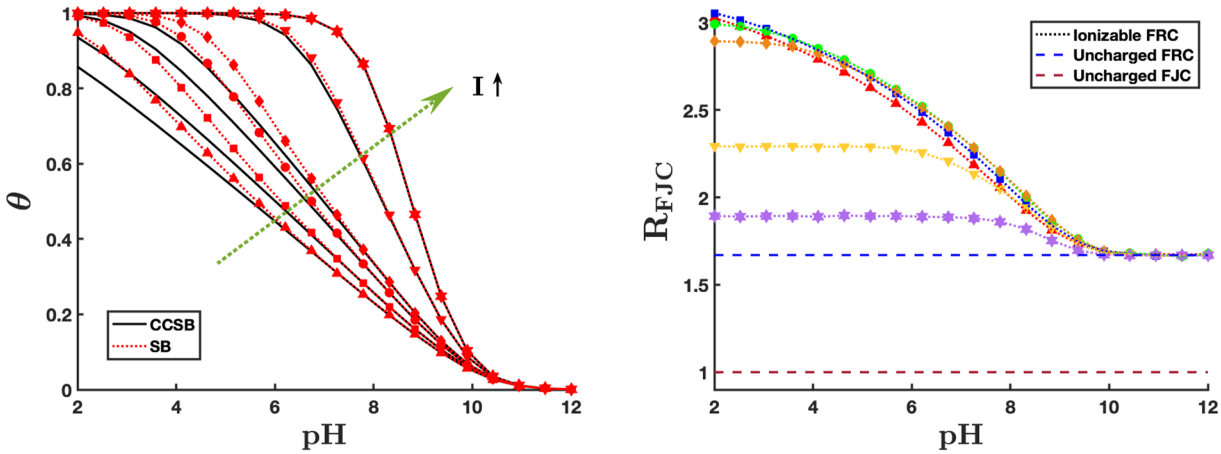

(a) $N = 20$

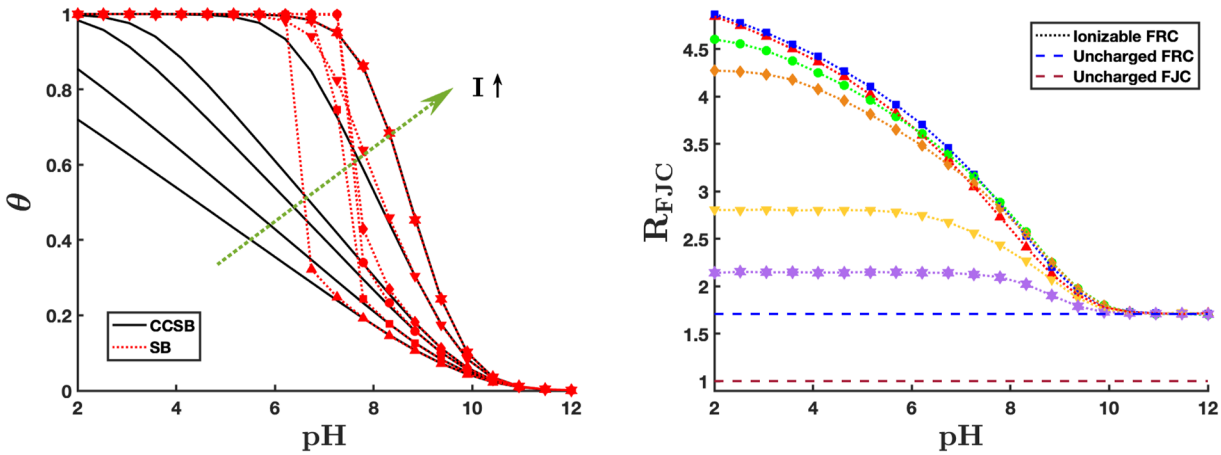

(b) $N = 50$

FIG. 8. Left panels: titration curves corresponding to a flexible ionizable FRC (black) and the equivalent rigid system considering up to triplet interactions (red). Right panels: normalized end-to-end distance vs the pH value. Chain lengths are (a) $N = 20$ and (b) $N = 50$ beads. For all the cases, $b = 0.25$ nm and $\log K = 9.0$. The ionic strengths used are 0.001M (upward triangles), 0.01M (squares), 0.05M (circles), 0.1M (diamonds), 1M (downward triangles), and 5M (stars). The end-to-end distance is normalized to that of the uncharged FJC, $R_{FJC} = \sqrt{\langle r^2\rangle/(N-1)b^2}$, and to improve data visibility, different colors have been used for each ionic strength. Dotted lines connecting the markers are shown only for guidance.

expressions are more involved (derivations and casuistry are provided in Sec. S-7.3 of the supplementary material). Triplets $\tilde{\lambda}_{ijk}$ only depend on the number of bonds linking the sites such as $\tilde{\lambda}_{ijk} = \tilde{\lambda}_{rs}$, where $r = |j - i|$ and $s = |k - j|$, which are plotted in Fig. 6(b). Interestingly, for the case $r, s \neq 1$, they are negative and therefore *attractive* so that they compensate the excess of repulsive pair energy interactions predicted by Eq. (16). Note that the decay to zero as r and s increase is very slow. As a result, when large chain flexibility is combined with electrostatic LR interactions, the SB free energy also converges very slowly.

As a consequence, the CCE convergence becomes problematic for long chains above some critical charge. In Fig. 7 (left panels), the titration curves obtained by SGCMC simulations (black lines) for the flexible chain are compared to the equivalent rigid system with pair and triplet interactions. It is observed that, although for the short chain ($N = 6$) the agreement is very good, a spurious jump takes place for the long chain ($N = 20$) below a critical pH-value, under which triplet interactions become important. Despite they are much less intense than pair interactions (for instance, an estimation for sites $i = 1$, $j = 3$, $k = 5$ yields a triplet interaction energy around 4% of the pair energy), their number scales very rapidly with N (as N^3 for the simulated chains). Since most of the triplet interactions are attractive, the degree of protonation jumps to full saturation.

Finally, note that the discrepancies between the flexible chain and the SB system are more prominent at intermediate ionic strengths, which can be explained as follows. For very high ionic strengths, the chain is very flexible, but SR interactions prevail so that, as already discussed in Sec. III, the SB model works. For very low ionic strengths, the chain becomes more rigid, the equivalent rigid system seems more suitable, and the jump appears at higher charges (lower pH-values). At intermediate ionic strengths, high flexibility and LR interactions collaborate and the CCE convergence becomes problematic even at very low degrees of ionization. Similar trends would be achieved modifying the permittivity ε of the solvent. Additional results (see Sec. S-7.4 of the supplementary material) show that introducing higher order interactions (quadruplets and quintuplets) makes the transition softer. However, from the experimental point of view, the use of such high order interactions becomes impractical.

One could argue that the problematic convergence of the CCE is due to the unrealistic large flexibility of the FJC model, while in real chains, monomers cannot overlap. In order to evaluate the effect of excluded volume, MC simulations have been performed and the titration curves were compared with the equivalent rigid system. The results are shown in Fig. 7(c). Although slightly softened, excluded volume does not prevent the formation of the spurious jump.

The simulated end-to-end distances are plotted in Fig. 7 (right panels). The FJC value is recovered at high pH-values, when the chain is uncharged. As the pH decreases, the chain swells until a certain saturation value, which strongly depends on the ionic strength, still far from the fully elongated chain (rod approximation). As expected, the lower the ionic strength, the larger the end-to-end distance is. We highlight that the chain swelling was already present in the case of SR interactions so that the chain flexibility is not the key factor in the convergence of the CCE, but only when it is combined with LR interactions.

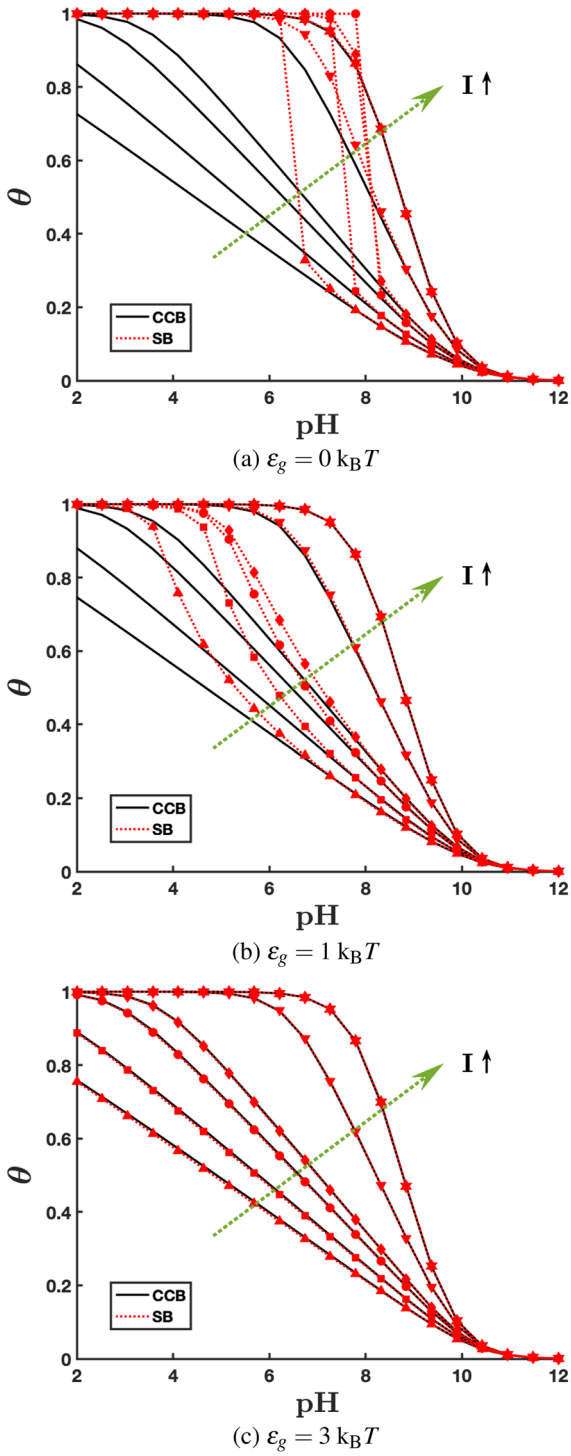

FIG. 9. Titration curves corresponding to a flexible ionizable RIS model (black) and the equivalent rigid system considering up to triplet interactions (red) for $N = 50$ and $\varepsilon_{g^+} = \varepsilon_{g^-} = 0$ (a), 1 (b), and 3 $k_B T$ (c). The parameters are $b = 0.25$ nm, $\gamma = 120°$, $\log K = 9.0$, and ionic strengths: 0.001M (upward triangles), 0.01M (squares), 0.05M (circles), 0.1M (diamonds), 1M (downward triangles), and 5M (stars). Dotted lines connecting the markers are shown only for eye guidance.

B. Freely Rotating Chain (FRC)

A similar analysis can be performed with more realistic chain models, which account for the rotational degrees of freedom of the bonds. In the simplest situation, the angle between adjacent bonds (bending angle) is fixed, while the dihedral formed by three consecutive bonds can rotate without restrictions. This is the so-called Freely Rotating Chain (FRC). Unlike the FJC model, no simple analytical expression is available for the distribution function $W(r_{ij})$. For this reason, the SB parameters have been obtained by performing the averages over the reference state as indicated in the CCEs [Eqs. (5)–(7)] by means of canonical MC simulations.

Although the FRC is significantly stiffer than the FJC, as indicated by larger values in the end-to-end distances (Fig. 8, right panel), the convergence of the CCE does not change significantly. Similar spurious jumps to those of the FJC case appear in the SB level with triplet interactions, although for larger N values. As observed in Fig. 8, the discontinuity is again present for $N = 50$ albeit not for $N = 20$. Simulations show that excluded volume effects do not change the situation significantly (provided as Sec. S-8.1 of the supplementary material).

C. Effect of rotational barriers: The Rotational Isomeric State (RIS) model

In real molecules, internal rotations around the bonds are not free due to the steric interaction among neighboring groups. Flory's idea was to replace the infinite number of rotational states by only those of minimum energy and more populated, namely *trans* (t), *gauche*$^+$ (g^+) and *gauche*$^-$ (g^-) (see Fig. 2). The result was the so-called Rotational Isomeric State (RIS) model.[64] Although he applied it to neutral molecules, an extension to weak PE was proposed in Refs. 13 and 17. The three states do not need to have the same energy, which results in varying degrees of chain stiffness. For instance, by increasing the *gauche* state energy, the *trans* state is preferred and the chain becomes more rigid.

As for the FRC, no known analytical expressions are available for the site–site distance distribution for the reference state. The results are depicted in Fig. 9. When the *trans* and *gauche* energies are the same [Fig. 9(a)], the obtained protonation curves are very similar to those of the FRC, and the spurious jump develops. However, as shown in Fig. 9(c), if the *gauche* states are hindered by increasing their energy ($\varepsilon_g = 3\ k_B T$ in this figure), the chain becomes much more rigid and the SB approach succeeds. Note, however, that the PE conformation is not completely locked at the all-*trans* conformation since, due to thermal fluctuations, the end-to-end distance does not achieve the contour length even at very low pH-values (see Sec. S-9.1 of the supplementary material).

V. CONCLUSIONS

The conformational and ionization equilibria of polyprotic molecules and flexible weak polyelectrolytes (PEs) are typically strongly coupled. Therefore, a combined treatment of protonation and conformation equilibria, referred to as the Coupled Conformational Site Binding (CCSB) level of description, becomes essential. In this article, we examine the effect of averaging (or "contracting") the conformational degrees of freedom, which transforms the original flexible molecule into an effective rigid object with identical ionization properties. This results in the Site Binding (SB) level of description, which is easier to handle both theoretically and computationally. In particular, the computational times are reduced by orders of magnitude, facilitating the use of standard fitting procedures to binding information.

The conformational averages involved can be systematically performed using proper Conformational Contraction Equations (CCEs). This work analyzes the conditions for the convergence of the CCE in the presence of both Short Range (SR) and Long Range (LR) electrostatic interactions. The main conclusions are summarized in the chart shown in Fig. 10.

First, we analyze two analytically solvable models based on the Freely Jointed Chain (FJC) with only SR interactions. In the first model, up to next-nearest neighbor, site–site interactions are taken into account, while the bonds are considered rigid. In the second model, the bonds can adopt two possible conformations, "short" and "long." When two consecutive bonds are both in a "short" conformation, an extra energy is added to the system.

In both models, despite significant chain flexibility, the SB free energy accurately reproduces the ionization properties. For independent bonds, the SB free energy is naturally truncated, allowing a very flexible chain to be *exactly* replaced by an effective rigid object with neighboring pairwise interactions. Generally, however, triplet and higher-order interactions arise at the SB level, which are analytically calculated.

The general picture changes when LR electrostatic interactions are included. If the polymer is stiff enough, the SB level of description still works very well. However, when LR interactions combine with high chain flexibility, the convergence of the CCE for long chains becomes problematic, leading to significant deviations from the CCSB titration curves. In some cases, spurious phase transitions in the protonation degree result when the SB free energy is truncated. The presence of excluded volume interactions or rotational restrictions does not alter the general picture either.

Finally, we highlight that, within the limitations discussed in this work, the SB approach can be regarded as a robust and useful technique, which greatly facilitates the analysis of the ionization equilibria in polyprotic molecules and polyelectrolytes, both at the theoretical and computational levels.

CHAIN FLEXIBILITY	INTERACTION TYPE	SB MODEL FEASIBILITY
LOW FLEXIBILITY	SR	✅
	SR + LR	✅
HIGH FLEXIBILITY	SR	✅
	SR + LR	⚠

FIG. 10. Outline showing the suitable conditions for the CCEs to converge, leading to an effective rigid system (SB model).

SUPPLEMENTARY MATERIAL

The supplementary material encompasses some derivations that could not be fitted into the main text due to lack of space. In addition, some results and figures covering a broader range of cases are also provided.

ACKNOWLEDGMENTS

P.M.B., S.M., and F.M. acknowledge the financial support from Generalitat de Catalunya (Grant No. 2021SGR00350). S.M. and F.M. acknowledge the Spanish Structures of Excellence María de Maeztu program through Grant No. CEX2021-001202-M. J.L.G. also acknowledges the Spanish Ministry of Science and Innovation (Project No. PID2022-140312NB-C21). P.M.B. acknowledges the financial support from the Spanish Ministry of Universities (Margarita Salas Grant No. MS98) and the funding from the European Union's Horizon Europe research and innovation program under the Marie Sklodowska-Curie Grant Agreement No. 101062456. J.O. acknowledges the financial support of the FPU21/05318 grant from the Spanish Ministry of Universities.

AUTHOR DECLARATIONS

Conflict of Interest

The authors have no conflicts to disclose.

Author Contributions

Javier Orradre: Conceptualization (equal); Data curation (lead); Formal analysis (equal); Investigation (lead); Methodology (lead); Software (equal); Validation (equal); Visualization (equal); Writing – original draft (equal); Writing – review & editing (equal). **Pablo M. Blanco**: Software (equal); Supervision (equal); Validation (equal); Visualization (equal); Writing – review & editing (equal). **Sergio Madurga**: Software (equal); Supervision (equal); Validation (equal); Visualization (equal); Writing – review & editing (equal). **Francesc Mas**: Conceptualization (equal); Funding acquisition (lead); Investigation (equal); Methodology (equal); Project administration (equal); Supervision (equal); Validation (equal); Visualization (equal); Writing – review & editing (equal). **Josep Lluís Garcés**: Conceptualization (lead); Data curation (equal); Formal analysis (lead); Investigation (equal); Methodology (equal); Supervision (equal); Validation (equal); Visualization (equal); Writing – original draft (equal); Writing – review & editing (equal).

DATA AVAILABILITY

The data that support the findings of this study are available from the corresponding author upon reasonable request.

REFERENCES

[1] B. Noszal and P. Sandor, "Rota-microspeciation of aspartic acid and asparagine," Anal. Chem. **61**, 2631–2637 (1989).
[2] M. Borkovec, B. Jonsson, and G. J. M. Koper, "Ionization processes and proton binding in polyprotic systems: Small molecules, proteins, interfaces, and polyelectrolytes," in *Surface and Colloid Science*, edited by E. Matijević (Springer, Boston, MA, 2001), pp. 99–339.
[3] M. Borkovec and G. J. Koper, "A cluster expansion method for the complete resolution of microscopic ionization equilibria from NMR titrations," Anal. Chem. **72**, 3272–3279 (2000).
[4] S. Madurga, M. Nedyalkova, F. Mas, and J. L. Garcés, "Ionization and conformational equilibria of citric acid: Delocalized proton binding in solution," J. Phys. Chem. A **121**, 5894–5906 (2017).
[5] R. A. Marcus, "Titration of polyelectrolytes at higher ionic strengths," J. Phys. Chem. **58**, 621–623 (1954).
[6] A. Katchalsky, "Polye1ectrolytes," Pure Appl. Chem. **26**, 327–374 (1971).
[7] M. Borkovec and G. J. M. Koper, "Ising models of polyprotic acids and bases," J. Phys. Chem. **98**, 6038–6045 (1994).
[8] M. Borkovec, J. Daicic, and G. J. M. Koper, "On the difference in ionization properties between planar interfaces and linear polyelectrolytes," Proc. Natl. Acad. Sci. U. S. A. **94**, 3499–3503 (1997).
[9] G. J. M. Koper and M. Borkovec, "Proton binding by linear, branched, and hyperbranched polyelectrolytes," Polymer **51**, 5649–5662 (2010).
[10] A. Ortega, D. Amorós, and J. García de la Torre, "Prediction of hydrodynamic and other solution properties of rigid proteins from atomic- and residue-level models," Biophys. J. **101**, 892–898 (2011).
[11] P. M. Blanco, S. Madurga, F. Mas, and J. L. Garcés, "Coupling of charge regulation and conformational equilibria in linear weak polyelectrolytes: Treatment of long-range interactions via effective short-ranged and pH-dependent interaction parameters," Polymers **10**, 811 (2018).
[12] P. M. Blanco, S. Madurga, F. Mas, and J. L. Garcés, "Effect of charge regulation and conformational equilibria in the stretching properties of weak polyelectrolytes," Macromolecules **52**, 8017–8031 (2019).
[13] P. M. Blanco, C. F. Narambuena, S. Madurga, F. Mas, and J. L. Garcés, "Unusual aspects of charge regulation in flexible weak polyelectrolytes," Polymers **15**(12), 2680 (2023).
[14] P. M. Blanco, S. Madurga, C. F. Narambuena, F. Mas, and J. L. Garcés, "Role of charge regulation and fluctuations in the conformational and mechanical properties of weak flexible polyelectrolytes," Polymers **11**, 1962 (2019).
[15] P. M. Blanco, S. Madurga, J. L. Garcés, F. Mas, and R. S. Dias, "Influence of macromolecular crowding on the charge regulation of intrinsically disordered proteins," Soft Matter **17**, 655–669 (2021).
[16] M. Stornes, P. M. Blanco, and R. S. Dias, "Polyelectrolyte-nanoparticle mutual charge regulation and its influence on their complexation," Colloids Surf., A **628**, 127258 (2021).
[17] J. L. Garcés, G. J. M. Koper, and M. Borkovec, "Ionization equilibria and conformational transitions in polyprotic molecules and polyelectrolytes," J. Phys. Chem. B **110**, 10937–10950 (2006).
[18] R. Fuoss, A. Katchalsky, and S. Lifson, "The potential of an infinite rod-like molecule and the distribution of the counter ions," Proc. Natl. Acad. Sci. U. S. A. **37**, 579–589 (1951).
[19] T. Alfrey, P. W. Berg, and H. Morawetz, "The counterion distribution in solutions of rod-shaped polyelectrolytes," J. Polym. Sci. **7**, 543–547 (1951).
[20] G. S. Manning, "Polyelectrolytes," Annu. Rev. Phys. Chem. **23**, 117–140 (1972).
[21] M. Ullner and B. Jonsson, "A Monte Carlo study of titrating polyelectrolytes in the presence of salt," Macromolecules **29**, 6645–6655 (1996).
[22] M. Ullner, B. Jönsson, B. Söderberg, and C. Peterson, "A Monte Carlo study of titrating polyelectrolytes," J. Chem. Phys. **104**, 3048–3057 (1996).
[23] M. Ullner, "Comments on the scaling behavior of flexible polyelectrolytes within the Debye–Hückel approximation," J. Phys. Chem. B **107**, 8097–8110 (2003).
[24] E. Companys, J. L. Garcés, J. Salvador, J. Galceran, J. Puy, and F. Mas, "Electrostatic and specific binding to macromolecular ligands: A general analytical expression for the Donnan volume," Colloids Surf., A **306**, 2–13 (2007).
[25] S. Madurga, J. L. Garcés, E. Companys, C. Rey-Castro, J. Salvador, J. Galceran, E. Vilaseca, J. Puy, and F. Mas, "Ion binding to polyelectrolytes: Monte Carlo simulations versus classical mean field theories," Theor. Chem. Acc. **123**, 127–135 (2009).
[26] T. L. Hill, "Approximate calculation of the electrostatic free energy of nucleic acids and other cylindrical macromolecules," Arch. Biochem. Biophys. **57**, 229–239 (1955).

[27]Y. Kawaguchi and M. Nagasawa, "Potentiometric titration of stereoregular poly(acrylic acids)," J. Phys. Chem. **73**, 4382–4384 (1969).
[28]G. S. Manning, "The molecular theory of polyelectrolyte solutions with applications to the electrostatic properties of polynucleotides," Q. Rev. Biophys. **11**, 179–246 (1978).
[29]P. I. Meyer, G. E. Wesenberg, and W. E. Vaughan, "Dielectric behavior of polyelectrolytes: II. The cylinder," Biophys. Chem. **13**, 265–273 (1981).
[30]V. Vlachy and D. A. McQuarrie, "A theory of cylindrical polyelectrolyte solutions," J. Chem. Phys. **83**, 1927–1932 (1985).
[31]G. V. Ramanathan, "Polyelectrolyte solutions with ionic mixtures," J. Chem. Phys. **85**, 2957–2960 (1986).
[32]T. Kitano, S. Kawaguchi, K. Ito, and A. Minakata, "Dissociation behavior of poly(fumaric acid) and poly(maleic acid). 1. Potentiometric titration and intrinsic viscosity," Macromolecules **20**, 1598–1606 (1987).
[33]D. Stigter, "Evaluation of the counterion condensation theory of polyelectrolytes," Biophys. J. **69**, 380–388 (1995).
[34]D. Stigter and K. A. Dill, "Binding of ionic ligands to polyelectrolytes," Biophys. J. **71**, 2064–2074 (1996).
[35]R. R. Netz and H. Orland, "Variational charge renormalization in charged systems," Eur. Phys. J. E **11**, 301–311 (2003).
[36]S. Buyukdagli and T. Ala-Nissila, "Electrostatic energy barriers from dielectric membranes upon approach of translocating DNA molecules," J. Chem. Phys. **144**, 084902 (2016).
[37]F. Oosawa, *Polyelectrolytes* (M. Dekker, 1971).
[38]P. M. Biesheuvel and M. A. Cohen Stuart, "Cylindrical cell model for the electrostatic free energy of polyelectrolyte complexes," Langmuir **20**, 4764–4770 (2004).
[39]M. Ullner, K. Qamhieh, and B. Cabane, "Osmotic pressure in polyelectrolyte solutions: Cell-model and bulk simulations," Soft Matter **14**, 5832–5846 (2018).
[40]J. Landsgesell and C. Holm, "Cell model approaches for predicting the swelling and mechanical properties of polyelectrolyte gels," Macromolecules **52**, 9341–9353 (2019).
[41]Y. Burak and R. R. Netz, "Charge regulation of interacting weak polyelectrolytes," J. Phys. Chem. B **108**, 4840–4849 (2004).
[42]R. L. Cleland, "Theory of potentiometric titration of polyelectrolytes: A discrete-site model for hyaluronic acid," Macromolecules **17**, 634–645 (1984).
[43]M. Ullner, B. Jönsson, and P.-O. Widmark, "Conformational properties and apparent dissociation constants of titrating polyelectrolytes: Monte Carlo simulation and scaling arguments," J. Chem. Phys. **100**, 3365–3366 (1994).
[44]A. Katchalsky, S. Lifson, and J. Mazur, "The electrostatic free energy of polyelectrolyte solutions. I. Randomly kinked macromolecules," J. Polym. Sci. **11**, 409–423 (1953).
[45]F. E. Harris and S. A. Rice, "The random chain model for polyelectrolytes," J. Polym. Sci. **15**, 151–156 (1955).
[46]C. E. Reed and W. F. Reed, "Monte Carlo study of titration of linear polyelectrolytes," J. Chem. Phys. **96**, 1609 (1992).
[47]A. V. Dobrynin, "Electrostatic persistence length of semiflexible and flexible polyelectrolytes," Macromolecules **38**, 9304–9314 (2005).
[48]J. L. Garcés, S. Madurga, and M. Borkovec, "Coupling of conformational and ionization equilibria in linear poly(ethylenimine): A study based on the site binding/rotational isomeric state (SBRIS) model," Phys. Chem. Chem. Phys. **16**, 4626–4638 (2014).
[49]R. G. Smits, G. J. M. Koper, and M. Mandel, "The influence of nearest- and next-nearest-neighbor interactions on the potentiometric titration of linear poly(ethylenimine)," J. Phys. Chem. **97**, 5745–5751 (1993).
[50]M. Borkovec, D. Čakara, and G. J. M. Koper, "Resolution of microscopic protonation enthalpies of polyprotic molecules by means of cluster expansions," J. Phys. Chem. B **116**, 4300–4309 (2012).
[51]V. V. Annenkov, V. A. Kruglova, and N. L. Mazyar, "Analysis of the potentiometric titration curves within the framework of the theory of the 'neighbor effect,'" J. Polym. Sci., Part B: Polym. Phys. **36**, 931–936 (1998).
[52]I. Borukhov, D. Andelman, R. Borrega, M. Cloitre, L. Leibler, and H. Orland, "Polyelectrolyte titration: Theory and experiment," J. Phys. Chem. B **104**, 11027–11034 (2000).
[53]G. Koper and M. Borkovec, "Binding of metal ions to polyelectrolytes and their oligomeric counterparts: An application of a generalized Potts model," J. Phys. Chem. B **105**, 6666–6674 (2001).
[54]A. Sadeghpour, A. Vaccaro, S. Rentsch, and M. Borkovec, "Influence of alkali metal counterions on the charging behavior of poly(acrylic acid)," Polymer **50**, 3950–3954 (2009).
[55]Z. Szakács, M. Kraszni, and B. Noszál, "Determination of microscopic acid-base parameters from NMR-pH titrations," Anal. Bioanal. Chem. **378**, 1428–1448 (2004).
[56]N. Metropolis, A. W. Rosenbluth, M. N. Rosenbluth, A. H. Teller, and E. Teller, "Equations of state calculations by fast computing machines," J. Chem. Phys. **21**, 1087–1091 (1953).
[57]W. K. Hastings, "Monte Carlo sampling methods using Markov chains and their applications," Biometrika **57**, 97–109 (1970).
[58]D. Chandler, *Introduction to Modern Statistical Mechanics* (Oxford University Press, 1987).
[59]J. Orradre, P. M. Blanco, S. Madurga, F. Mas, and J. L. Garces, "Exact solution for a general FJC polyelectrolyte model with up to next nearest neighbour interactions," arXiv:2406.03991 (2024).
[60]G. J. M. Koper and M. Borkovec, "Exact affinity distributions for linear polyampholytes and polyelectrolytes," J. Chem. Phys. **104**, 4204–4213 (1996).
[61]M. Nagasawa, T. Murase, and K. Kondo, "Potentiometric titration of stereoregular polyelectrolytes," J. Phys. Chem. **69**, 4005–4012 (1965).
[62]L. R. G. Treloar, "The statistical length of long-chain molecules," Trans. Faraday Soc. **42**, 77–82 (1946).
[63]P. J. Flory, *Statistical Mechanics of Chain Molecules* (Wiley, 1969).
[64]P. J. Flory and R. L. Jernigan, "Second and fourth moments of chain molecules," J. Chem. Phys. **42**, 3509–3519 (1965).